Spin Electronics

Finite Element Modeling of Charge- and Spin-Currents in Magnetoresistive Pillars With Current Crowding Effects

N. Strelkov[1,2], A. Vedyayev[1,2], D. Gusakova[1,3], L. D. Buda-Prejbeanu[1], M. Chshiev[1*], S. Amara[1], A. Vaysset[1], and B. Dieny[1**]

[1] SPINTEC, UMR-8191, CEA-INAC/CNRS/UJF-Grenoble 1/Grenoble-INP, 17 rue des martyrs, 38054 Grenoble Cedex 9, France
[2] Department of Magnetism, Faculty of Physics, Lomonosov University, Moscow, Russia
[3] CEA-LETI, MINATEC, DRT/LETI/DIHS/LCRF, 38054 Grenoble, France
[*] Member, IEEE
[**] Senior Member, IEEE

Received 25 June 2010, accepted 12 July 2010, published 15 September 2010.

Abstract—Charge- and spin-diffusion equations, taking into account spin-diffusion and spin-transfer torque, were numerically solved using a finite element method in complex noncollinear geometry. As an illustration, this approach was used to study the spin-dependent transport in a two-dimensional model giant magnetoresistance metallic pillar sandwiched between extended electrodes as is the case in magnetoresistive heads for hard disk drives. In this model system, the charge current crowding around the boundaries between the electrodes and the pillar has a quite significant influence on the spin current within the magnetoresistive pillar.

Index Terms—Spin electronics, magnetoresistive devices, giant magnetoresistance, tunnelling magnetoresistance, spin polarized transport.

I. INTRODUCTION

Spin electronics was born in 1988 with the discovery of giant magnetoresistance (GMR) [Baibich 1988, Binasch 1989]. Since then, it has been expanding due to a strong synergy between fundamental research and industrial developments particularly concerning magnetoresistive heads for hard disk drives [Dieny 1991, Vedyayev 1997], magnetic random access memory [Durlam 2003], logic devices [Matsunaga 2008] and RF oscillators [Houssameddine 2007]. Most of these spintronic devices under research and development involve inhomogeneous current flows. This is the case in metallic pillars or low-resistance tunnel junctions implying current crowding effects [Chen 2002], in point contact RF oscillators [Kaka 2005], in GMR current-perpendicular-to-plane (CPP) magnetoresistive heads and especially in current confined path structures [Nagasaka 2001, Fukuzawa 2004]. To quantitatively interpret experimental data in these complex geometries or to design spintronic devices with nonuniform current flow, it is therefore important to develop a theoretical tool, which is able to describe the spin-dependent transport (charge- and spin-currents) as well as spin-transfer torques in systems of arbitrary shape and magnetic configuration.

The purpose of the present study was to develop such a tool in the case of diffusive transport. In this letter, we present our approach to accomplish this goal and apply it to the calculation of the transport properties in a two-dimensional (2-D) model CPP-GMR pillar sandwiched between extended electrodes. We show that the current crowding effect, which takes place in such structure gives rise to quite peculiar spin transport phenomena.

Corresponding author: B. Dieny (bernard.dieny@cea.fr).
Digital Object Identifer: 10.1109/LMAG.2010.2069556

II. METHOD

The general formalism that we used in the diffusion limit is derived based on the extension of Valet and Fert theory to noncollinear geometry [Valet 1993, Zhang 2002]. Each material constituting the system of arbitrary shape and composition is described by local transport parameters (C_0−conductivity, β−spin asymmetry of C_0, N_0−density of states at Fermi level).

All transport properties are then described by four local variables: the scalar electrostatic potential $\tilde{\varphi}$ and the three components of spin accumulation in spin-space (m_x, m_y, m_z). The local charge current vector is then given by the following:

$$\mathbf{j}^e = 2C_0\nabla\tilde{\varphi} - \frac{2\beta C_0}{eN_0}(\mathbf{u}_M, \nabla\mathbf{m}) \tag{1}$$

where $\mathbf{u}_M$ is a unit vector parallel to the local magnetization and e is the electron charge. The spin current is described by a tensor (three coordinates in spin space, three coordinates in real space) and expressed as follows:

$$\mathbf{j}^m = \frac{2\hbar\beta C_0}{e}\mathbf{u}_M\nabla\tilde{\varphi} - \frac{2C_0}{e^2N_0}\nabla\mathbf{m}. \tag{2}$$

The four variables are then calculated everywhere in space in steady state by numerically solving the two fundamental equations of spin-dependent diffuse transport (four scalar equations).

$$\begin{cases} \operatorname{div}\mathbf{j}^e = 0 & (3) \\ \operatorname{div}\mathbf{j}^m + \dfrac{J_{sd}}{\hbar}(\mathbf{m}\times\mathbf{u}_M) + \dfrac{\mathbf{m}}{\tau_{sf}} = 0 & (4) \end{cases}$$

where J_{sd} and τ_{sf}, respectively, represent the *s*–*d* exchange interaction energy and the spin relaxation time; $\hbar$ is the Planck constant.

The first equation expresses the conservation of charge. The second one states that the spin polarization of the current is not conserved. It can vary either because of spin relaxation or

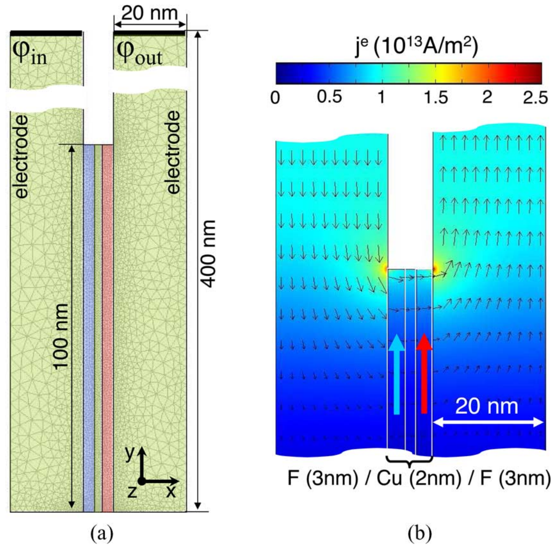

Fig. 1. (a) Scheme of studied magnetoresistive nanopillar sandwiched between two extended electrodes. The nanopillar composition is a model sandwich of the form F3 nm/Cu2 nm/F3 nm in which F is a ferromagnetic metal. For F, we used bulk parameters corresponding to those of Co [Fert 1999]: $C_0 = 0.005\ \Omega^{-1}$ nm^{-1}, $\beta = 0.6$, $l_{sf} = 20$ nm, $\lambda_J = 1$ nm. For the nonmagnetic layers and the outer electrode, we used the parameters known for Cu: $C_0 = 0.02\ \Omega^{-1}$ nm^{-1}, $l_{sf} = 50$ nm. (b) Zoom on the magnetoresistive nanopillar showing the electron flow (arrows) and charge current amplitude (color map).

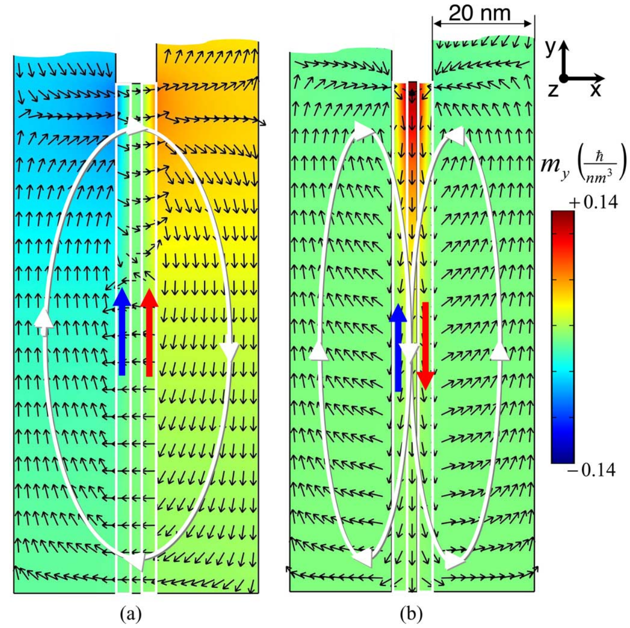

Fig. 2. Zoom around the magnetoresistive pillar showing the y-component of spin current flow throughout the system in (a) parallel magnetic configuration, (b) antiparallel configuration. The normalized arrows indicate the spin current flow, whereas the color map represents the y-component of the spin accumulation. Here, we assume that the majority spins in ferromagnetic are aligned with magnetization vector.

because of the local spin-transfer torque, which induces a precession of the spin accumulation around the local magnetization due to s–d exchange interaction. The spin-transfer torque itself is given by $\mathbf{T} = \left(J_{sd}/\hbar\right)(\mathbf{m} \times \mathbf{u}_M)$.

The constants τ_{sf} and J_{sd} are related to two characteristic lengths l_{sf} and λ_J, respectively. The first one is the spin-diffusion length $l_{sf} = \sqrt{2(1-\beta^2)D_0\tau_{sf}}$, where D_0 represents the diffusion constant, while another one is written as $\lambda_J = \sqrt{2\hbar D_0/J_{sd}}$ and represents the spin-reorientation length, i.e., the distance over which the spin polarization gets reoriented along the local magnetization. In addition, at outer boundaries, we impose no perpendicular component of charge- and spin-current except at the boundaries where a potential is applied.

III. RESULTS

Using this general formalism adapted for the finite element solver, the spatial distribution of the charge- and spin-currents as well as the spin transfer torque (STT) was calculated in a model 2-D magnetoresistive nanopillar sandwiched between two nonmagnetic extended metallic electrodes, as shown in Fig. 1(a). The nanopillar consists of two 3-nm-thick magnetic layers (reference and free layers) separated by a 2 nm thick nonmagnetic metallic spacer. Its height is 100 nm. We assume that the relative orientation of the magnetizations in the two magnetic layers can be varied in the plane perpendicular to x-axis. Voltages of, respectively, $\varphi_{\text{in}} = 0$ V and $\varphi_{\text{out}} = 50$ mV are uniformly applied between the top surfaces of the two electrodes. In this model study, we only considered bulk spin-dependent scattering and bulk spin relaxation. Interfacial scattering could also be introduced by describing each interface as a thin layer having bulk properties matching the interfacial spin-dependent scattering properties. Taking into account interfacial scattering would not change the qualitative description of the phenomena presented in this paper. The bulk parameters that we used for the various materials are representative of the case of Co and Cu [Fert 1999]. Under these assumptions, the resistance of the stack in parallel (antiparallel) configuration for the magnetizations of the adjacent magnetic layers is found to be $R_P = 802$ Ω/nm ($R_{AP} = 806$ Ω/nm) per unit length in the z-direction (i.e., crosstrack in a head geometry) yielding a magnetoresistance $\Delta R/R_P = 0.5\%$.

Fig. 1(b) shows the charge current flow through the device (arrows) and the charge current amplitude (color map) throughout the structure in parallel magnetic configuration. Because the charge current is trying to follow the shortest path throughout the structure, it has a pronounced vertical gradient within the magnetoresistive pillar. The current amplitude is actually ten times larger in the upper part of the pillar than in its bottom part. Hot spots are visible around the upper corners of the pillar.

Fig. 2 shows the spin-current distribution (arrows) of the spin component parallel to the y-axis, i.e., to the magnetization of the reference layer, for two magnetic configurations: parallel [see Fig. 2(a)] and antiparallel [see Fig. 2(b)]. The color map represents the y-component of the spin accumulation.

In the parallel case [see Fig. 2(a)], the electrons, which are initially unpolarized in the Cu electrodes, get more and more polarized as they approach the magnetic pillar. Since the charge current is much more intense in the upper part of the pillar

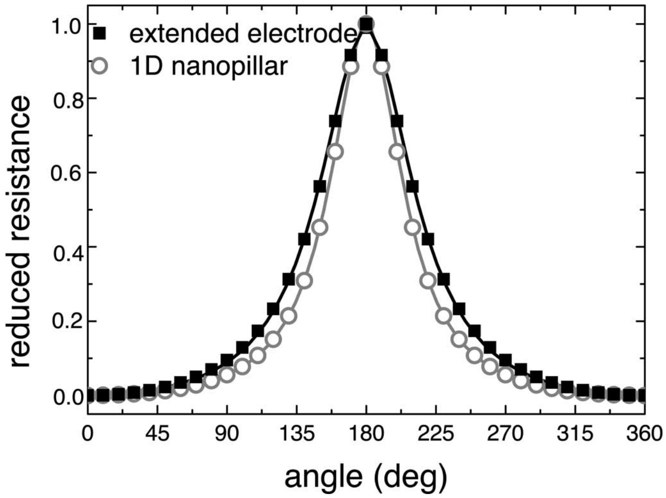

Fig. 3. Comparison of angular variation of CPP-GMR in the present nanopillar sandwiched between extended electrode (black squares) and throughout the same nanopillar assuming uniform current flow in x-direction –1-D model (gray circles).

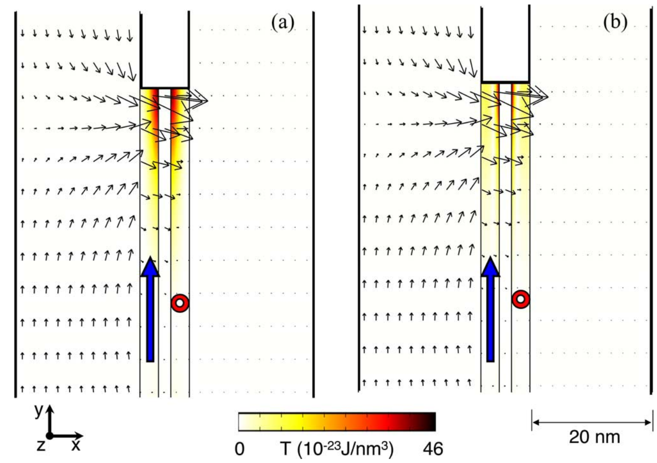

Fig. 4. (a) In-plane and (b) perpendicular-to-plane components of spin transfer torque in 90° magnetic configuration. The black arrows represent the y-component of spin current, whereas the color map is associated with the STT amplitude.

compared to that in the lower part, the y-component of spin current is also much more intense in the upper part of the pillar than in its lower part. Correlatively, a large excess of electron spin aligned with negative y-axis arises in the Cu electrode on the left-hand side of the pillar. Symmetrically, an excess of electron spins aligned with positive y-axis appears in the Cu electrode on the right-hand side of the pillar. These excess densities of polarized electrons are largest on both sides of the upper part of the pillar, as indicated in Fig. 2(a), and are minimal around the bottom part of the structure. As a result of this distribution of spin accumulation, a vortex of diffusion spin current is formed as represented by the white arrows in Fig. 2(a). Unexpectedly, this implies that the y-component of spin current has opposite directions in the upper and lower parts of the magnetoresistive pillar, and that the spin current is opposite to the charge current in the lower part of the pillar.

The situation in antiparallel configuration is quite different [see Fig. 2(b)]. The y-component of spin accumulation is now maximum in the nonmagnetic spacer layer but is much larger in the upper part of the pillar than in its lower part due to the vertical gradient in charge current density. The resulting gradient of y-component of spin accumulation gives rise to an intense in-plane y-component of spin current flowing in the spacer layer as well as two symmetric vortices of y-component of spin current flowing in the Cu electrodes on both sides of the pillar, as indicated by white arrows in Fig. 2(b).

Fig. 3 shows the reduced resistance $r = [R(\theta) - R(0)] / [R(\pi) - R(0)]$ versus the angle between the magnetizations of the two magnetic layers in two situations: 1) the aforementioned nanopillar sandwiched between two extended electrodes and 2) the same nanopillar sandwiched between two electrodes extending along the x-direction and having the same cross section as the pillar so that the charge current is uniform throughout the stack (1-D model with charge current flowing along x-axis).

Clearly, the angular variation of CPP-GMR does not follow a simple cosine variation, which is in agreement with theoretical expectation [Slonczewski 2002]. Furthermore, it follows from Fig. 3 that the system geometry influences the angular variation. This further emphasizes the need to take into account the influence of spatial current nonuniformities in the design of spintronic devices.

As a further step, we show in Fig. 4(a) and (b) the in-plane (Slonczewski's torque term [Slonczewski 1996]) and perpendicular-to-plane (field-like term [Zhang 2002]) components of STT in 90° magnetic configuration. The black arrows represent the y-component of spin current, whereas the color map is related to the STT amplitude. As already pointed out for metallic pillars [Zhang 2002], the perpendicular component of the torque is much smaller (by more than 1 order of magnitude) than the in-plane component. Furthermore, since the charge current density is much higher in the upper part of the pillar than in its bottom part, the STT amplitude is also much larger in the upper part of the pillar. From the viewpoint of magnetization dynamics, this implies that magnetic excitations due to STT are likely to be first generated in the upper part of the pillar as the current density is increased above the STT excitation threshold.

IV. CONCLUSION

A numerical tool has been developed to compute the charge- and spin-current in magnetic structures of arbitrary shape and composition. This tool has been used to investigate the spin-dependent transport properties through magnetoresistive nanopillars sandwiched between extended electrodes. It was shown that the current crowding effect gives rise to strong in-plane inhomogeneities in spin accumulation yielding large in-plane components of spin current. This type of tool should be quite helpful in the design of functional spintronic devices as well as for the quantitative interpretation of experimental data in devices with nonuniform or nonlocal currents. As a next step, the computation of the micromagnetic dynamics will be self-consistently coupled to these calculations of transport properties.

ACKNOWLEDGMENT

This work was supported in part by the European RTN "Spinswitch" MRTN-CT-2006–035327, in part by the Chair of Excellence Program of the Nanosciences Foundation (Grenoble, France), and in part by the ERC Advanced Grant "HYMAGINE." NS and AV are grateful to the SPINTEC Laboratory for hospitality and RFBR for partial financial support. DG acknowledges the French National Research Agency (ANR) (CARNOT program). This work has been presented in invited talk EA-06 at Intermag 2009 in Sacramento, California.

REFERENCES

Baibich M N, Broto J M, Fert A, Nguyen Van Dau F, Petroff F (1988), "Giant magnetoresistance of (001)Fe/(001)Cr magnetic superlattices," *Phys. Rev. Lett.*, vol. 61, pp. 2472–2475, doi: 10.1103/PhysRevLett.61.2472.

Binasch G, Grünberg P, Saurenbach F, Zinn W (1989), "Enhanced magnetoresistance in layered magnetic structures with antiferromagnetic interlayer exchange," *Phys. Rev. B*, vol. 39, pp. 4828–4830, doi: 10.1103/PhysRevB.39.4828.

Chen J, Li Y, Nowak J, Fernandez de Castro J (2002), "Analytical method for two dimensional current crowding effect in magnetic tunnel junctions," *J. Appl. Phys.*, vol. 91, pp. 8783–8785, doi: 10.1063/1.1452654.

Dieny B, Speriosu V S, Parkin S S P, Gurney B A, Wilhoit D R, Mauri D (1991), "Giant magnetoresistive in soft ferromagnetic multilayers," *Phys. Rev. B*, vol. 43, pp. 1297–1300, doi: 10.1103/PhysRevB.43.1297.

Durlam M, Naji P J, Omair A, DeHerrera M, Calder J, Slaughter J M, Engel B N, Rizzo N D, Grynkewich G, Butcher B, Tracy C, Smith K, Kyler K W, Ren J J, Molla J A, Feil W A, Williams R G, Tehrani S (2003), "A 1-Mbit MRAM based on 1T1MTJ bit cell integrated with copper interconnects," *IEEE J. Solid State Circuits*, vol. 38, pp. 769–773, doi: 10.1109/JSSC.2003.810048.

Fert A, Piraux L (1999), "Magnetic nanowires," *J. Magn Magn. Mater.*, vol. 200, pp. 338–358, doi: 10.1016/S0304-8853(99)00375-3.

Fukuzawa H, Yuasa H, Hashimoto S, Koi K, Iwasaki H, Takagishi M, Tanaka Y, Sahashi M (2004), "MR ratio enhancement by NOL current-confined-path structures in CPP spin valves," *IEEE Trans. Magn.*, vol. 40, pp. 2236–2238, doi: 10.1109/TMAG.2004.829185.

Houssameddine D, Ebels U, Delaët B, Rodmacq B, Firastrau I, Ponthenier F, Brunet M, Thirion C, Michel J-P, Prejbeanu-Buda L, Cyrille M-C, Redon O, Dieny B (2007), "Spin-torque oscillator using a perpendicular polarizer and a planar free layer," *Nature Mater.*, vol. 6, pp. 447–453, doi: 10.1038/nmat1905.

Kaka S, Pufall M R, Rippard W H, Silva T J, Russek S E, Katine J A (2005) *Nature (London)*, vol. 437, pp. 389–392, doi: 10.1038/nature04035.

Matsunaga S, Hayakawa J, Ikeda S, Miura K, Hasegawa H, Endoh T, Ohno H, Hanyu T (2008), "Fabrication of a nonvolatile full adder based on logic-in-memory architecture using magnetic tunnel junctions," *Appl. Phys. Expr.*, vol. 1, 091301, doi: 10.1143/APEX.1.091301.

Nagasaka K, Seyama Y, Varga L, Shimizu Y, Tanaka A (2001), "Giant magnetroresistance properties of specular spin valve films in a current perpendicular to plane structure," *J. Appl. Phys.*, vol. 89, pp. 6943–6945, doi: 10.1063/1.1364636.

Slonczewski J C (1996), "Current-driven excitation of magnetic multilayers," *J. Magn. Magn. Mater.*, vol. 159, pp. L1–L7, doi: 10.1016/0304-8853(96)00062-5.

Slonczewski J C (2002), "Currents and torques in metallic magnetic multilayers," *J. Magn. Magn. Mater.*, vol. 247, pp. 324–338, doi: 10.1016/S0304-8853(02)00291-3.

Valet T, Fert A (1993), "Theory of the perpendicular magnetoresistance in magnetic multilayers," *Phys. Rev. B*, vol. 48, pp. 7099–7113, doi: 10.1103/PhysRevB.48.7099.

Vedyayev A, Chshiev M, Ryzhanova N, Dieny B, Cowache C, Brouers F (1997), "A unified theory of CIP and CPP giant magnetoresistance in magnetic sandwiches," *J. Magn. Magn. Mater.*, vol. 172, pp. 53–60, doi: 10.1016/S0304-8853(97)00081-4.

Zhang S, Levy P M, Fert A (2002), "Mechanisms of spin-polarized current-driven magnetization switching," *Phys. Rev. Lett.*, vol. 88, 236601, doi: 10.1103/PhysRevLett.88.236601.